Multi-labeled Random-forest Enabled Softwarized Management for Photonics Switching Systems

Photonics Integrated Multiband WSS Based ROADM Architecture: A Networking Analysis

Muhammad Umar Masood
Politecnico di Torino, IT
muhammad.masood@polito.it

Lorenzo Tunesi
Politecnico di Torino, IT
lorenzo.tunesi@polito.com

Bruno Correia
Politecnico di Torino, IT
bruno.dearaujo@polito.it

Ihtesham Khan
Politecnico di Torino, IT
ihtesham.khan@polito.it

Enrico Ghillino
Synopsys, USA
enrico.ghillino@synopsys.com

Paolo Bardella
Politecnico di Torino, IT
paolo.bardella@polito.it

Andrea Carena
Politecnico di Torino, IT
andrea.carena@polito.it

Vittorio Curri
Politecnico di Torino, IT
curri@polito.it

***Abstract*—The modern idea of connectivity and the progress in bandwidth-intensive applications requires expanding the Internet's capacity. The technologies like spatial-division multiplexing (SDM) and band-division multiplexing (BDM) have emerged as viable options for boosting the capacity of existing wavelength-division multiplexing (WDM) optical systems in the C-band and accommodating growing traffic requirements. This paper proposes a network-level analysis of novel modular photonic integrated multiband wavelength selective switch (WSS) architecture (operate on S+C+L bands) for a reconfigurable optical add-drop multiplexer (ROADM) operation. The networking analysis of the proposed WSS switching fabric is performed on the USA network for the SDM and BDM scenarios. The assessment is based on the channel allocation of the fiber in both the SDM and BDM cases. Promising results are achieved, showing that the proposed WSS has the capability to fully utilize the potentiality of the cost-effective BDM approach and enhance the network capacity without installing new fiber infrastructure as compared to the SDM solution, which requires the deployment of additional fiber for capacity augmentation.**

***Index Terms*—Multiband, Wavelength Selective Switch, Photonic Integrated Circuit, High-capacity Optical Systems**

I. Introduction

Internet traffic is expected to grow at a compound annual growth rate (CAGR) of 30% worldwide [1]. Apart from Internet access, which is supported by wireless technologies, with the full deployment of 5G technology enabling a significant increase in capacity, all other network components will rely on optical transmission over fiber infrastructures. To address this, network operators must formulate affordable, scalable, and adaptable strategies to expand the capacity of the current infrastructure. Coherent optical technologies with dual polarization spanning the whole C-band in a spectral range of 4.8 THz are typically used in modern optical transport. This allows for a transmission range throughput of roughly 38.4 Tbps per fiber while employing PM-16QAM [2].

Various solutions must be implemented, either by scaling the currently in use technologies or implementing new ones, to further increase the network's capacity. In this scenario, the first solution is SDM which could be implemented utilizing multicore (MCF), multimode (MMF), or multi-parallel (MPF) fibers. The other solution in this direction is BDM, which utilizes a broader spectrum of the fiber and aims to permit transmission over the whole low-loss spectrum of optical fibers (e.g., 54 THz in ITU G.652.D fiber). These two are the best practical choices for extending the capacity of optical networks. Only MPF, out of all SDM-based options, is currently available commercially; it relies on the presence of dark fibers or the installation of new ones. This strategy is made possible by emulating the established and economic C-band line system technology. The remaining SDM alternatives (such as MCF and MMF, for example) offer a great deal of potential to boost transmission capacity, but doing so necessitates a thorough overhaul of the optical transport ecosystem because it calls for the installation of new fibers and equipment. This requirement is unfavorable due to the high capital costs for short- or medium-term applications. BDM, on the other hand, is the most practical short-term solution to enhance the capacity of optical networks because it may maximize the return on investment of an already established optical infrastructure.

The primary step toward the practical implementation of the BDM approach is the development of filtering and switching modules that enable transparent wavelength routing. In this context, the key role of the network element, WSS, offers independent control and routing of every input channel to a fiber output of the WDM comb. Generally, microelectromechanical mirrors (MEMS) and liquid crystal on silicon (LCoS) technology are used to construct bulky WSS systems.

The primary step toward the practical implementation of the BDM approach is the development of filtering and switching modules that enable transparent wavelength routing. In this context, the key role of the network element, WSS, offers independent control and routing of every input channel to a fiber output of the WDM comb. Generally, microelectromechanical mirrors (MEMS) and liquid crystal on silicon (LCoS) technology are used to construct bulky WSS systems.

On the other hand, this work suggests a multi-band WSS implementation using the fastly developing photonic integrated circuits (PIC) technology, which offers a low-cost solution with a compact footprint and high production capacity. The proposed WSS's modular architecture allows it to function throughout a wide portion of the optical spectrum, including

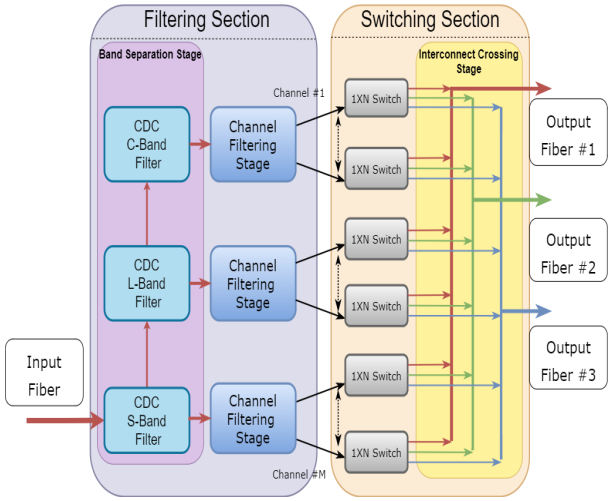

Fig. 1: General architecture of the WSS.

the S+C+L bands. In comparison to traditional MEMS-based systems, the suggested WSS's design allows for flexibility for additional output fibers and a large number of channels with a smaller footprint. The local add/drop module of the ROADM is not considered in this analysis; only the switching functionality of the ROADM architecture (WSS module) is considered. A detailed network performance assessment of the proposed ROADM architecture based on the new multi-band WSS is also demonstrated, comparing SDM and BDM solutions on the USA network.

II. Wavelength Selective Switch Architecture

Wavelength Selective Switches are devices able to independently route each channel of a given input signal towards any of the target ports: these devices must be designed to keep loss, signal-degradation, and cross-talk to a minimum. The proposed structure has been therefore designed based on a divide-and-conquer approach: by separating the WDM comb de-multiplexing and the switching operation into multiple stages, the components can be designed with higher accuracy and precision. Overall the architecture can be divided into two stages, as shown in Fig. 1, namely the filtering and the switching stages. The first step of the filtering stage consists of separating the three bands of operation (S+C+L), which are then routed to separate channel de-multiplexer modules. The next blocks are highlighted in Fig. 2: the WDM combs of the three bands are divided into their individual channels by a cascade of filters, which are then propagated to an independent $1\times N$ switching network, tasked with routing each channel to the target output port (1-N). The connection between the output of the switching networks and the ports of the device is achieved through a waveguides crossings stage, which can be modeled as a passive section. This parallel cascaded structure can be described through two main parameters, namely the number of channels (M) and the number of output ports of the device (N): given a desired (M,N) application, the filtering and switching stages can be adapted to provide the required circuit size while maintaining the independence of the previous sub-blocks.

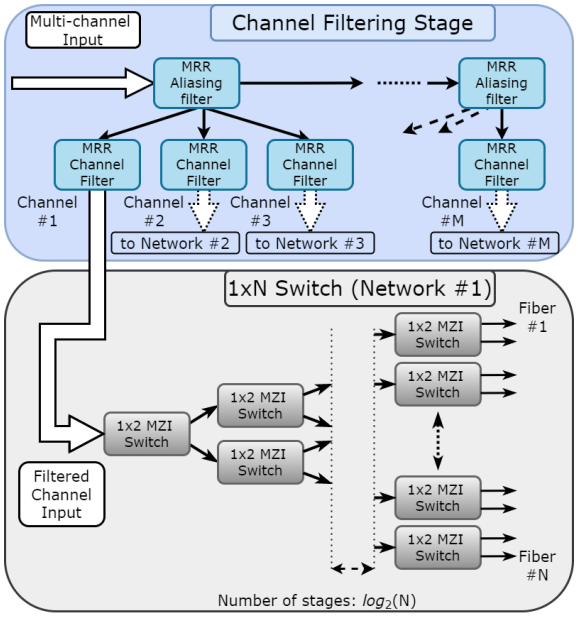

Fig. 2: Highlights of the internal topology for the channel filtering and switching.

III. Device Modelling

A variety of simulation and mathematical model have been used to evaluate and design the frequency response of the component, using methods ranging from Beam Propagation Method, Coupled Mode Theory and Finite Difference Time Domain models, available in the Synopsys Photonic Simulation Suite. All the required operations can be achieved by using three fundamental devices, namely Contra-Directional Couplers (CDCs), Micro-Ring Resonators (MRRs) and Mach-Zehnder Interferometers (MZIs). The initial band separation has been carried out through CDC [3], due to their large flat filtering bandwidth and steep-roll off: such elements are needed in order to both minimize the inter-band crosstalk, as well as reduce the number of cascaded channel filters, dividing the comb into three independent pathways. Once this first operation is achieved the individual channel extraction is carried out using two-stage ladder MRR filters [4], which can be designed to achieve flat-top narrow filtering bandwidths, necessary for dense WDM applications. Additional anti-aliasing MRR-based elements have been modeled to further reduce the inter-channel crosstalk. The switching networks are then modeled using standard thermally-controlled MZI as basic Optical Switching Elements (OSEs), able to provide low-loss frequency-independent switching [5], [6]. The waveguide crossing interconnects have instead been considered as lossy, frequency-independent elements (L=0.045 dB) [7]. All these elements have been simulated and characterized as block models, allowing full-scale simulation of the system to extract the QoT metrics.

IV. WDM Transport Layer Simulations

The complete WSS model has been characterized in a DSP coherent simulation environment, using the OptSim© Photonic

Circuit Simulation Suite. The proposed data is presented for a 40 channel implementation scenario, using channel spacing FSR=100 GHz and N=3 possible output fibers. The channels have been considered as 16-QAM modulated, with a symbol rate R_s = 60 GBaud and operating on the 400ZR standard [8]. The QoT impairments were characterized through Optical Signal-to-Noise Ratio penalty (ΔOSNR), using the Bit-Error Rate (BER) extracted from the simulation for a threshold $BER_{th}=10^{-3}$ [9]. The OSNR penalty of the device is composed of two major contributions: the path-independent filtering and switching and the path-dependent number of encountered crossings. The path-independent effect can be simulated without taking the routing into account, as the channel experience this loss independently from the applied switch control. The crossings penalty must instead be evaluated for all the possible paths that each channel can traverse. Furthermore, given the non-negligible path dependence effect, the penalty can be estimated based on the topology of the interconnect stage which can be evaluated based only on the M and N parameters. The simulation results have been depicted to highlight this phenomenon, as shown in Fig. 3, which shows the average and the variance of the measured QoT impairments of the channel as a function of the number of encountered crossings. Overall the device is shown to behave compatibly in the three bands of interest, with similar flat penalties for every channel, and a straightforward model for the path-dependant impairment evaluation.

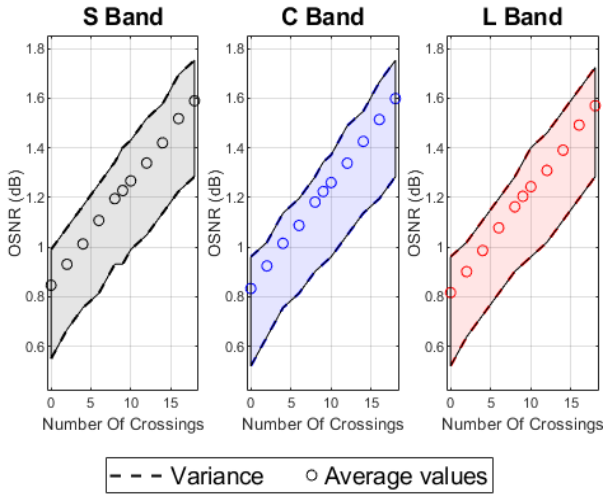

Fig. 3: Simulated OSNR penalty in the S+C+L regions.

This relationship can be used to build a generalized model which can allow the investigation of larger and smaller implementations (M,N) without requiring full-scale DSP simulations. In this context, the worst path penalty can be seen as the main figure of merit regarding the device scalability (Fig. 4). The topological-based abstraction can be considered as a reasonable trade-off between penalty estimation and computational time. The rigorous DSP simulation is carried out for a reasonable test implementation, using the extracted data to virtually characterize different M and N topologies.

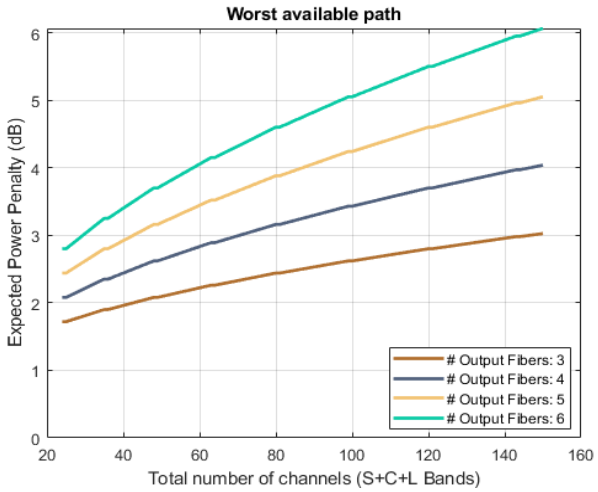

Fig. 4: Penalty estimation as a function of the device scale.

V. Network Performance Evaluation

We studied the network's overall performance to assess the impact of the new WSS architecture on various optical transport solutions. We employed the Statistical Network Assessment Process (SNAP) tool [10], which operates on the tested network's physical layer and is based on the degradation in QoT brought on by each component of the network. The generalized signal-to-noise ratio (GSNR) is used here as the QoT metric and is derived using both the P_{ASE} and P_{NLI}.

$$\mathrm{GSNR_i} = \frac{P_{\mathrm{S,i}}}{P_{\mathrm{ASE}(f_i)} + P_{\mathrm{NLI,i}}(f_i)}\,, \tag{1}$$

for the ith channel with center frequency f_i, where $P_{\mathrm{S,i}}$ is the transmitted power of the signal.

We suppose a multi-band optical line system, constructed for three bands with network components, particularly optical amplifiers, that are optimized for each band. Therefore, we assume that all of the amplified lines' fibers have identical 75 km lengths and that the type of fibers being utilized is standard single-mode fiber (ITU-T G.652D). For the C- and L-band channels, we consider the use of commercially available erbium-doped fiber amplifiers (EDFAs), and for the S-band, we consider the use of thulium-doped fiber amplifiers. The ZR+ transceivers tuned on a symbol rate of 60 Gbaud are used to operate each band on the ITU-T 100 GHz WDM grid. Using a span-by-span approach and the local optimization global optimization (LOGO) algorithm [11], the input power is optimized for each band having 40 channels per band. Additionally, the routing and wavelength assignment (RWA) method (k shortest pathways with $k_{max} = 5$ for routing and first-fit for spectrum allocation) is used to assign the lightpaths (LPs). Furthermore, a uniform traffic distribution among the network nodes is used to conduct the network assessment. This study took into account the USA topology, which consists of 43 edges and 24 optical nodes, and Monte Carlo analysis is used to determine network metrics statistically.

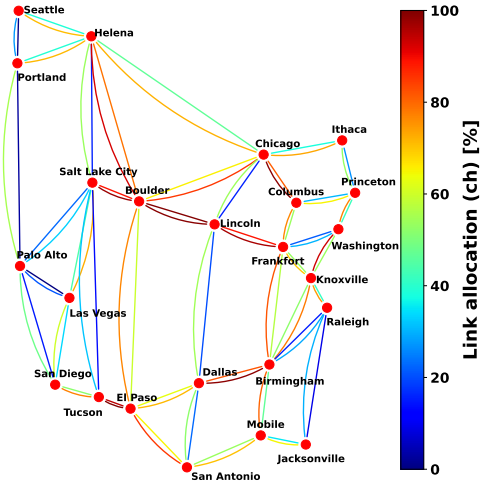

(a) SDM (C-band, 2x fibers, 40 ch/fiber)

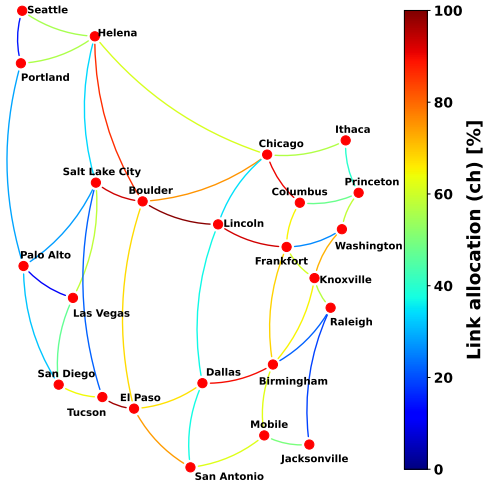

(b) BDM (C+L-band, 1x fiber, 80 ch/fiber)

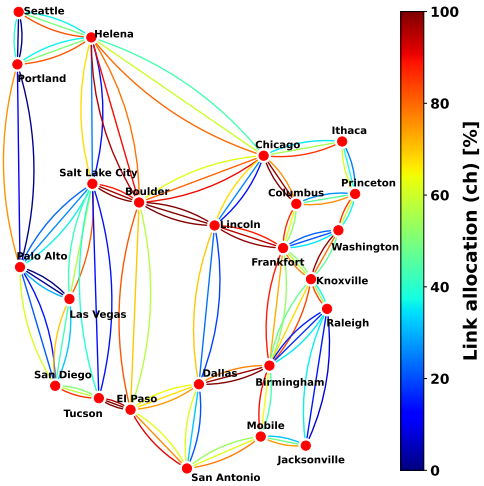

(c) SDM (C-band, 3x fibers, 40 ch/fiber)

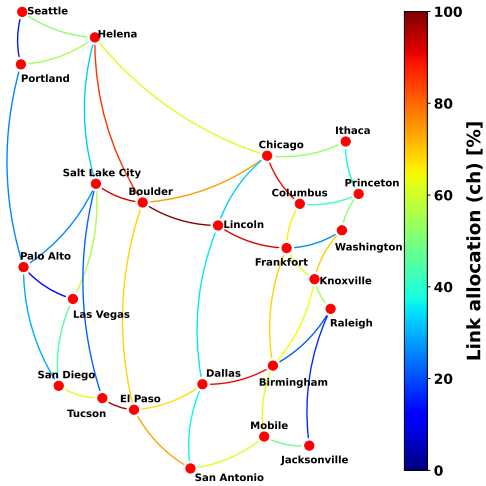

(d) BDM (S+C+L-band, 1x fibers, 120 ch/fiber)

Fig. 5: Channel allocation comparison - ZR+ transceiver.

VI. Results and Conclusion

In order to evaluate the multiband outcomes when integrating the ROADM architecture with the suggested WSS structure, we compare the performance of the BDM network with that of the SDM network to ensure a fair benchmark. We performed the SNAP network performance analysis assuming SDM with multiple fibers in the C-band on the same total spectrum. For SDM, we consider a core continuity constraint (CCC), where each LP must be assigned in the same fiber from the source to the destination node, following the switching technique [12]. In our analysis, the SDM approach uses multiples fiber (2x and 3x) compared to the BDM approach. These multiples are taken into account to make a fair comparison between the link capacities of SDM (C-band only) and BDM (C+L and S+C+L bands).

The analysis is done with respect to channel allocation (40 channels/band) in both the SDM with multiple fibers and BDM scenarios. Fig. 5 (a) and (b) shows the comparison between SDM (2x fibers) and BDM (C+L, 80 channels/fiber), whereas Fig. 5 (c) and (d) shows the comparison of SDM (3x fibers) with BDM (S+C+L). The channel allocations per fiber link are represented in the form of a heat map (percentage) from 0%(blue) - 100%(orange). The channels utilized for the overall network in Fig. 5 (a) is 55.65% for the SDM case (2x fibers, C-band only, 40 channels/fiber), whereas the channel utilization in Fig. 5 (b) is 55.46% for the BDM case (1x fiber, C+L band, 80 channels/link). For Fig. 5 (c), the channel utilization is 56.72% for the SDM case (3x fibers, C-band only, 40 channels/fiber), whereas for the BDM case (1x fiber, S+C+L bands, 120 channels/fiber) the channel utilization is 54.25% for the overall network. For both scenarios, the channel allocation in the BDM scenario is slightly lower than in the SDM scenario, while the difference between SDM and BDM increases in the case of SDM (3x fiber) and BDM

(S+C+L bands) due to the nonlinear propagation caused by the transmission of all three bands.

In any case, the link allocation difference observed in the BDM scenario is small, suggesting that BDM solutions are a potentially cost-effective way to upgrade network capacity without installing new fiber.

REFERENCES

[1] Cisco, "VNI complete forecast highlights," https://bit.ly/3oXh37T (2022).

[2] K. Kim, K.-H. Doo, H. H. Lee, S. Kim, H. Park, J.-Y. Oh, and H. S. Chung, "High speed and low latency passive optical network for 5g wireless systems," Journal of Lightwave Technology **37**, 2873–2882 (2018).

[3] M. Hammood *et al.*, "Broadband, silicon photonic, optical add–drop filters with 3 dB bandwidths up to 11 THz," Opt. Lett. **46**, 2738–2741 (2021).

[4] A. P. Masilamani and V. Van, "Design and realization of a two-stage microring ladder filter in silicon-on-insulator," Opt. Express **20**, 24708–24713 (2012).

[5] X. Tu *et al.*, "State of the art and perspectives on silicon photonic switches," Micromachines **10** (2019).

[6] I. Khan *et al.*, "Optimized management of ultra-wideband photonics switching systems assisted by machine learning," Opt. Express **30**, 3989–4004 (2022).

[7] M. Johnson *et al.*, "Low-loss, low-crosstalk waveguide crossing for scalable integrated silicon photonics applications," Opt. Express **28**, 12498–12507 (2020).

[8] Implementation agreement for a 400ZR coherent optical interface, https://www.oiforum.com/technical-work/hot-topics/400zr-2/.

[9] I. Khan *et al.*, "Performance evaluation of data-driven techniques for softwarized and agnostic management of N×N photonic switch," Opt. Continuum **1** (2022).

[10] V. Curri, M. Cantono, and R. Gaudino, "Elastic all-optical networks: A new paradigm enabled by the physical layer. How to optimize network performances?" J. Light. Technol. **35**, 1211–1221 (2017).

[11] V. Curri, A. Carena, A. Arduino, G. Bosco, P. Poggiolini, A. Nespola, and F. Forghieri, "Design strategies and merit of system parameters for uniform uncompensated links supporting Nyquist-WDM transmission," J. Light. Technol. **33**, 3921–3932 (2015).

[12] P. S. Khodashenas, J. M. Rivas-Moscoso, D. Siracusa, F. Pederzolli, B. Shariati, D. Klonidis, E. Salvadori, and I. Tomkos, "Comparison of spectral and spatial super-channel allocation schemes for sdm networks," J. Light. Technol. **34**, 2710–2716 (2016).